Inorg. Chem. **2004**, *43*, 5704–5713

Synthesis, Structure, and Catalytic Properties of V^{IV}, Mn^{III}, Mo^{VI}, and U^{VI} Complexes Containing Bidentate (N, O) Oxazine and Oxazoline Ligands

Karuppasamy Kandasamy,[†] Harkesh B. Singh,*[,†] Ray J. Butcher,[‡] and Jerry P. Jasinski[§]

Departments of Chemistry, Indian Institute of Technology, Bombay, Powai, Mumbai 400 076, India, Howard University, Washington, D.C. 20059, and Keene State College, Keene, New Hampshire 03435-2001

Received October 22, 2003

Synthesis of seven complexes containing oxazoline {$[(L_1)_2V{=}O]$ (**4**), $[(L_1)_2MoO_2]$ (**5**), $[(L_1)_2UO_2]$ (**6**); HL_1 (**1**) [HL_1 = 2-(4′,4′-dimethyl-3′-4′-dihydroxazol-2′-yl)phenol]}, chiral oxazoline {$[(L_2)_2UO_2]$ (**7**); HL_2 (**2**) [HL_2 = (4′*R*)-2-(4′-ethyl-3′4′-dihyroxazol-2′-yl)phenol]}, and oxazine {$[(L_3)_2V{=}O]$ (**8**), $[(L_3)_2Mn(CH_3COO^-)]$ (**9**), $[(L_3)_2Co]$ (**10**); HL_3 (**3**) [HL_3 = 2-(5,6-dihydro-4*H*-1,3-oxazolinyl)phenol]} and their characterization by various techniques such as UV–vis, IR, and EPR spectroscopy, mass spectrometry, cyclic voltammetry, and elemental analysis are reported. The novel oxazine (**3**) and complexes **4**, **5**, **8** and **9** were also characterized by X-ray crystallography. Oxazine **3** crystallizes in the monoclinic system with the $P2_1/n$ space group, complexes **4** and **9** crystallize in the monoclinic system with the $P2_1/c$ space group, and complexes **5** and **8** crystallize in the orthorhombic system with the $C222_1$ space group and the $P2_12_12_1$ chiral space group, respectively. The representative synthetic procedure involves the reaction of metal acetate or acetylacetonate derivatives with corresponding ligand in ethanol. Addition of $Mn(OAc)_2{\cdot}4H_2O$ to an ethanol solution of **3** gave the unexpected complex $Mn(L_3)_2{\cdot}(CH_3COO^-)$ (**9**) where the acetate group is coordinated with the metal center in a bidentate fashion. The catalytic activity of complexes **4**–**9** for oxidation of styrene with *tert*-butyl hydroperoxide was tested. In all cases, benzaldehyde formed exclusively as the oxidation product.

Introduction

The chemistry of oxazoline-based ligands continues to be an area of interest due to their use as chirality-transfer auxiliaries in combination with several transition metals in a wide range of asymmetric catalytic reactions.[1] Several metal complexes bearing 2-(2′-hydroxyphenyl)oxazolines have been reported in the literature.[2] Of particular interest is the use of chiral copper(II) complexes with 2-(2′-hydroxyphenyl)oxazolines in asymmetric Bayer−Villiger reactions.[3] In recent years, other metal complexes such as oxo−vanadium,[4] oxo−molybdenum,[5] oxo−rhenium,[6] and manganese[7] with such types of ligands have been demonstrated as efficient catalysts in oxygen transfer reactions. Pd(II)[8] and Cu(I)[9] oxazoline complexes have been employed

* To whom correspondence should be addressed. E-mail: chhbsia@chem.iitb.ac.in.
[†] Indian Institute of Technology.
[‡] Howard University.
[§] Keene State College.

(1) (a) Rechavi, D.; Lemaire, M.; *Chem. Rev.* **2002**, *102*, 3467. (b) Johnson, J. S.; Evans, D. A. *Acc. Chem. Res.* **2000**, *33*, 325. (c) Pfaltz, A. *Acc. Chem. Res.* **1993**, *26*, 339. (d) Ghosh, A. K.; Mathivanan, P.; Cappiello, J. *Tetrahedron: Asymmetry* **1998**, *9*, 1. (e) Bolm, C.; Luong, T. K. K.; Schlingloft, G. *Synlett.* **1997**, 1151. (f) Bolm, C.; Bienewald, F.; Schlingloft, G. *J. Mol. Catal.* **1997**, *117*, 347. (g) Bolm, C.; Bienewald, F.; Harms, K. *Synlett.* **1996**, 775. (h) Pfaltz, A. *Adv. Catal. Processes* **1995**, *1*, 61 and references therein. (i) Bolm, C.; Bienewald, F. *Angew. Chem., Int. Ed. Engl.* **1995**, *34*, 2640. (j) Moreno, R. M.; Bueno, A.; Moyano, A. *J. Organomet. Chem.* **2003**, *671*, 187.

(2) (a) Braunstein, P.; Naud, F. *Angew. Chem., Int. Ed.* **2001**, *40*, 680. (b) Bolm, C. *Angew. Chem., Int. Ed. Engl.* **1991**, *30*, 542. (c) Gómez, M.; Muller, G.; Rocamora, M. *Coord. Chem. Rev.* **1999**, *193*−*195*, 769. (d) Gómez-Simón, M.; Jansat, S.; Muller, G.; Panyella, D.; Font-Bardia, M.; Solans, X. *J. Chem. Soc., Dalton Trans.* **1997**, 3755−3764. (e) Cozzi, P. G.; Floriani, C.; Chiesi-Villa, A.; Rizzoli, C. *Inorg. Chem.* **1995**, *34*, 2921. (f) Cozzi, P. G.; Gallo, E.; Floriani, C.; Chiesi-Villa, A.; Rizzoli, C. *Organometallics* **1995**, *14*, 4994. (g) Gant, T. G.; Meyers, A. I. *Tetrahedron* **1994**, *50*, 2297.

(3) (a) Bolm, C.; Schlingloff, G. *J. Chem. Soc., Chem. Commun.* **1995**, 1247. (b) Bolm, C.; Schlingloff, G.; Weickhardt, K. *Angew. Chem., Int. Ed. Engl.* **1994**, *33*, 1848; *Tetrahedron Lett.* **1993**, *34*, 3405. (c) Peng, Y.; Feng, X.; Yu, K.; Li, Z.; Jiang, Y.; Yeung, C.-H. *J. Organomet. Chem.* **2001**, *619*, 204.

(4) (a) Bolm, C.; Luong, T. K.; Harms, K. *Chem. Ber./Recl.* **1997**, *130*, 887. (b) Hwang, J. J. H.; Abu-Omar, M. M. *Tetrahedron Lett.* **1999**, *40*, 8313.

(5) Gómez, M.; Jansat, S.; Muller, G.; Noguera, G.; Teruel, H.; Moliner, V.; Cerrada, E.; Hursthouse, M. *Eur. J. Inorg. Chem.* **2001**, 1071.

(6) Arias, J.; Newlands, C. R.; Abu-Omar, M. M. *Inorg. Chem.* **2001**, *40*, 2185.

10.1021/ic0352093 CCC: $27.50 © 2004 American Chemical Society
Published on Web 08/03/2004

in cyclopropanation reactions. Recently, oxo−rhenium complexes have been utilized as efficient catalysts for the reduction of perchlorate with sulfides under mild condition.[10] Control of the stereoselectivity of the catalytic process of these complexes mainly depends on the steric or electronic nature of the ligands around the metal center.[5,7,11]

Very recently, our group reported the coordination studies of Mn, Co, Ni, Cu, and Zn with 2-(4′,4′-dimethyl-3′-4′-dihydroxazol-2′-yl)phenol.[12] The behavior of the manganese and nickel acetates toward 2-(4′,4′-dimethyl-3′,4′-dihydro-oxazol-2′-yl)phenol was very unusual and quite interesting compared with that of the other reported oxazolines. In the manganese complex, one of the oxazoline rings was partially hydrolyzed in the presence of the acetic acid eliminated during the reaction whereas the expected 1:2 or 1:3 manganese complexes were reported in a similar kind of reactions.[2d,7] When the reaction was carried out with $Ni(OAc)_2 \cdot 4H_2O$, tetra- and hexacoordinated complexes were obtained. In the hexacoordinated complex, two acetic acid molecules were coordinated in addition to the two bidentate oxazoline ligands. In continuation of our work, we have now undertaken the task of preparing oxo−metal complexes containing oxazoline ligands **1** and **2** as the oxo−metal complexes having oxazoline moieties are still quite limited[4a,5,6,10,13] and systematic studies on their structural and reactivity patterns have not been carried out. In particular, no examples of oxo−uranium complexes with any oxazoline moiety have been reported, although uranium−oxide based materials are used as catalysts for the destruction of volatile chloro−organic compounds.[14]

In view of the fact that the steric modulation on the ligands mainly affects various properties of their complexes, we have also designed a novel ligand (**3**) having a six-membered bidentate (N,O) oxazine moiety and undertaken its complexation studies to find out the influence of the ring size (steric) effect on the structural and catalytic properties, and we compared these with those of the complexes containing five-membered oxazoline moieties. It would also be interesting to compare the nature of the interaction between nitrogen and metal atoms which may be affected due to the absence of methyl groups on the carbon atom adjacent to the nitrogen in the oxazine ring (electronic effect) owing to the possibility of resonance structures (Chart 1). In this paper, we report the synthesis and characterization, both in solution and in the solid state, of new oxo−vanadium, oxo−molybdenum, and the first examples of oxo-uranium complexes with **1** and **2**. We also report the novel ligand **3**, and its oxo−vanadium, manganese, and cobalt complexes. Also, we have tested the ability of these complexes for oxidation of styrene. Structural comparison of the oxo−vanadium complex of **3** with corresponding complexes of five-membered oxazoline moieties, in particular with the complexes of **1** and **2**, is attempted. It will be worth mentioning that the synthesis and coordination studies of oxazine (**3**) with any metal have not been reported in the literature to date.

Chart 1

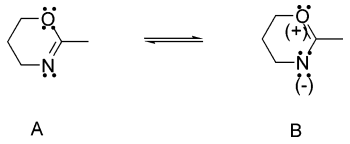

A B

Experimental Section

General Procedures. All reactions were performed under inert atmosphere using Schlenk techniques. All solvents were purified by the standard procedures[15] and were freshly distilled prior to use. All chemicals, e.g., 2-hydroxy benzonitrile (Lancaster) and amino alcohols (Lancaster), were purchased and used without further purification. The oxazoline (**1** and **2**) and oxazine (**3**) ligands were synthesized using the reported procedure with slight modification.[16] Infrared spectra were taken on a Nicolet Impact 400 spectrophotometer with samples prepared as KBr pellets. Solution electronic absorption spectra were collected on a Shimadzu UV-160A spectrophotometer. Cyclic voltammetric experiments were conducted using CH1600A electrochemical analyzer. All experiments were carried out under inert atmosphere in acetonitrile solution with 0.1 M tetrabutylammonium perchlorate or tetrabutylammonium bromide or tetrabutylammonium hexafluorophosphate as a supporting electrolyte. Cyclic voltammograms (CVs) were obtained using a standard three-electrode cell consisting of glassy carbon (working), platinum (auxiliary), and SCE (standard) electrodes. Potentials are reported versus a Ag/AgCl (KCl saturated) couple using a $[Fe(C_5H_5)_2]^+/[Fe(C_5H_5)_2]$ redox couple as an internal standard. ^1H and ^{13}C NMR spectra were recorded on a Varian VXR 300S spectrometer operating at 300 and 75.42 MHz, respectively. EPR spectra of the complexes in dichloromethane were recorded with a Varian E-112 EPR spectrometer using tetracyanoethylene as g marker ($g = 2.00277$) at room temperature as well as at liquid nitrogen temperature. Elemental analyses were performed on a Carlo-Erba model EA 1112 CHNS analyzer. ES-MS spectra were recorded at room temperature on a Q-TOF micro (YA-105) mass spectrometer. Fast atomic bombardment (FAB) mass spectra were recorded at room temperature on a JEOL SX 102/DA-6000 mass spectrometer/data system with xenon (6 kV, 10 mV) as the

(7) (a) Hoogenraad, M.; Kooijman, H.; Spek, A. L.; Bouwman, E.; Haasnoot, J. G.; Reedijk, J. *Eur. J. Inorg. Chem.* **2002**, 2897. (b) Hoogenraad, M.; Ramkisoensing, K.; Gorter, S.; Driessen, W. L.; Bouwman, E.; Haasnoot, J. G.; Reedijk, J.; Mahabiersing, T.; Hartl, F. *Eur. J. Inorg. Chem.* **2002**, 377. (c) Hoogenraad, M.; Ramkisoensing, K.; Driessen, W. L.; Kooijman, H.; Spek, A. L.; Bouwman, E.; Haasnoot, J. G.; Reedijk, J. *Inorg. Chim. Acta* **2001**, *320*, 117. (d) Hoogenraad, M.; Ramkisoensing, K.; Kooijman, H.; Spek, A. L.; Bouwman, E.; Haasnoot, J. G.; Reedjik, J. *Inorg. Chim. Acta* **1998**, *279*, 217.
(8) Miller, K. J.; Baag, J. H.; Abu-Omar, M. M. *Inorg. Chem.* **1999**, *38*, 4510.
(9) Đaković, S.; Liščić-Tumir, L.; Kirin, S. I.; Vinković, V.; Raza, Z.; Šuste, A.; Šunjić, V. *J. Mol. Catal. A: Chem.* **1997**, *18*, 27.
(10) Abu-Omar, M. M.; McPherson, L. D.; Arias, J.; Béreau, V. M. *Angew. Chem., Int. Ed.* **2000**, *39*, 4310.
(11) Pfaltz, A. *Acta Chem. Scand.* **1996**, *50*, 189.
(12) Mugesh, G.; Singh, H. B.; Butcher, R. J. *Eur. J. Inorg. Chem.* **2001**, 669.
(13) Melchior, M.; Thompson, K. H.; Jong, J. M.; Rettig, S. J.; Shuter, E.; Yuen, V. G.; Zhou, Y.; McNeill, J. H.; Orvig, C. *Inorg. Chem.* **1999**, *38*, 2288.
(14) Hutchings, G. J.; Heneghan, C. S.; Hudson, I. D.; Taylor, S. H. *Nature* **1996**, *384*, 341.
(15) Perrin, D. D.; Armargo, W. L. F.; Perrin, D. R. *Purification of Laboratory Chemicals*; Pergamon: New York, 1980.
(16) (a) Serrano, J. L.; Sierra, T.; González, Y.; Bolm, C.; Weickhardt, K.; Magnus, A.; Moll, G. *J. Am. Chem. Soc.* **1995**, *117*, 8312. (b) Bolm, C.; Weickhardt, K.; Zehnder, M.; Ranff, T. *Chem. Ber.* **1991**, *124*, 1173.

bombarding gas. The accelerating voltage was 10 kV. *m*-Nitrobenzyl alcohol was used as the matrix with cation detection. For isotopes, the value given is for the most intense peak. GC analyses were performed on a Shimadzu GC-15A gas chromatograph. Optical rotations were measured by a JASCO model DIP 370 digital polarimeter.

Synthesis of HL_3 (3). 3-Amino-1-propanol (5.1 mL, 67.2 mmol), 2-hydroxy benzonitrile (5.34 g, 44.9 mmol), and $ZnCl_2$ (0.306 g, 2.24 mmol) were dissolved in chlorobenzene and refluxed for 24 h under inert atmosphere. The reaction mixture was filtered and evaporated to give a brown oil. It was dissolved in dichloromethane and washed three times with water. The organic extract was separated, dried over Na_2SO_4, filtered, and evaporated under reduced vacuum to give the desired compound as a white solid. Colorless crystals were obtained by recrystallization from dichloromethane. Yield: 70%. Mp 78−80 °C. Anal. Calcd for $C_{10}H_{11}NO_2$: C, 67.78; H, 6.26; N, 7.90. Found: C, 67.52; H, 6.26; N, 8.11. Selected IR frequency (KBr disk, cm^{-1}) = 1637(s, $\nu_{C=N}$). Electronic absorption spectrum in CH_2Cl_2 λ_{max} (nm) (ϵ (M^{-1} cm^{-1})): 314 (19380). ^1H NMR (300 MHz, $CDCl_3$, δ): 2.00 (p), 3.56 (t), 4.36 (t), 6.76−7.76 (m), 14.17 (s). ^{13}C NMR (300 MHz, $CDCl_3$, δ): 21.5, 40.7, 65.2, 114.5, 117.1, 117.5, 126.6, 132.3, 159.3, 160.9. GC-MS (*m*/*z*): 177 (M^+).

$[(L_1)_2V{=}O]$ (4). To an ethanol solution (40 mL) of vanadium acetylacetonate (0.265 g, 1 mmol) was added ligand **1** (0.38 g, 2 mmol) dissolved in 10 mL of the same solvent. The violet color changed into blackish brown after complete addition of **1**. After 24 h stirring at room temperature, the solution was filtered and evaporated under reduced vacuum to give the desired compound. Recrystallization from the mixture of dichloromethane and hexane (1:3) gave violet crystals. Yield: 0.156 g, 35%. Mp 228−230 °C. Anal. Calcd for $C_{22}H_{24}N_2O_5V$: C, 59.06; H, 5.40; N, 6.26. Found: C, 59.11; H, 5.36; N, 6.14. Selected IR frequencies (KBr disk, cm^{-1}) 1617 ($\nu_{C=N}$), 995 ($\nu_{V=O}$). Electronic absorption spectrum in CH_2Cl_2 λ_{max} (nm) (ϵ (M^{-1} cm^{-1})): 540−550 (33), 600−620 (50), 800−850 (59), and 325−330 (8100). ESR (dichloromethane, 77 and 298 K): g_{av} = 1.9777 and A_{av} = 100. ES-MS (*m*/*z*): 447 (M^+).

$[(L_1)_2MoO_2]$ (5). An ethanol (10 mL) solution of **1** (0.38 g, 2 mmol) was added to the solution (40 mL) of $MoO_2(acac)_2$ (0.326 g, 1 mmol) in the same solvent. After 24 h stirring at room temperature, the solution was filtered and evaporated under reduced vacuum to give the desired yellow compound. Yellow crystals were obtained from acetonitrile. Yield: 0.376 g, 37%. Mp (decomposes) >218 °C. Anal. Calcd for $C_{22}H_{24}MoN_2O_6$: C, 51.98; H, 4.76; N, 5.51. Found: C, 51.74; H, 4.50; N, 5.32. Selected IR frequencies (KBr disk, cm^{-1}): 1622 ($\nu_{C=N}$), 919 ($\nu_{Mo=O}$). Electronic absorption spectrum in DMSO λ_{max} (nm) (ϵ (M^{-1} cm^{-1})): 296 (1070). ^1H NMR (300 MHz, DMSO-d_6, δ): 0.81 (t), 0.88 (t), 1.60−2.40 (m), 4.20 (d), 4.40 (m), 4.70 (m), 6.00 (d), 6.60 (t), 6.80−7.20 (m), 7.40 (m), 7.60 (d). ^{13}C NMR (300 MHz, DMSO-d_6, δ): 26.7, 28.0, 66.7, 77.8, 110.2, 116.3, 118.9, 120.6, 127.6, 133.6, 159.0, 162.9.

$[(L_1)_2UO_2]$ (6). To an ethanol solution (40 mL) of $UO_2(OAc)_2$ (0.468 g, 1 mmol) was added ligand **1** (0.38 g, 2 mmol) dissolved in 10 mL of the same solvent. The solution immediately changed color from yellow to orange. After 24 h stirring at room temperature, the solution was filtered and evaporated under vacuum to give the desired compound as an orange solid. Recrystallization from the mixture of acetonitrile and hexane (1:2) gave an orange crystalline solid. Yield: 0.16 g, 25%. Mp 140−142 °C. Anal. Calcd for $C_{22}H_{24}N_2O_6U$: C, 40.62; H, 3.72; N, 4.31. Found: C, 40.41; H, 3.71; N, 4.20. Selected IR frequencies (KBr disk, cm^{-1}): 1627 ($\nu_{C=N}$), 909 ($\nu_{U=O}$). Electronic absorption spectrum in CH_2Cl_2 λ_{max} (nm) (ϵ (M^{-1} cm^{-1})): 305 (17710). ^1H NMR (300 MHz, $CDCl_3$, δ): 1.0 (t), 2.2 (s), 2.6 (s), 4.1 (t), 4.2 (t), 4.5 (t), 4.8 (t), 5.0 (s), 7−8 (m). ^{13}C NMR (300 MHz, $CDCl_3$/DMSO-d_6, δ): 27.0, 28.1, 66.7, 80.7, 110.4, 116.1, 117.5, 118.3, 127.6, 132.9, 133.7, 159.3. MS (ES, *m*/*z*): 650 (M^+).

$[(L_2)_2UO_2]$ (7). To an ethanol solution (40 mL) of $UO_2(OAc)_2$ (0.468 g, 1 mmol) was added ligand **2** (0.38 g, 2 mmol) dissolved in 10 mL of the same solvent. After 24 h stirring at room temperature, the solution was filtered and evaporated under vacuum to give the desired compound. Recrystallization from the mixture of acetonitrile and hexane (1:2) gave an orange crystalline solid. Yield: 0.26 g, 40%. Mp 127−129 °C. Anal. Calcd for $C_{22}H_{24}N_2O_6U$: C, 40.62; H, 3.72; N, 4.31. Found: C, 40.48; H, 3.68; N, 4.18. Selected IR frequencies (KBr disk, cm^{-1}): 1627 ($\nu_{C=N}$), 909 ($\nu_{U=O}$). Electronic absorption spectrum in CH_2Cl_2 λ_{max} (nm) (ϵ (M^{-1} cm^{-1})): 306 (10959), 350 (5163). ^1H NMR (300 MHz, $CDCl_3$, δ): 1.4 (s), 4.2(s), 7−8 (m). ^{13}C NMR (300 MHz, $CDCl_3$/DMSO-d_6, δ): 8.5, 10.0, 27.3, 28.6, 66.5, 71.4, 72.4, 114.6, 116.5, 117.7, 118.5, 120.4, 127.9, 129.9, 133.1, 134.5, 160.0, 160.9, 170.4, 170.7. FAB-MS (*m*/*z*): 650 (M^+). $[\alpha]^{25}_D$ +2.5° (*c* 1, EtOH).

$[(L_3)_2V{=}O]$ (8). To an ethanol solution (40 mL) of $VO(acac)_2$ (0.265 g, 1 mmol) was added ligand **3** (0.355 g, 2 mmol) dissolved in 10 mL of the same solvent. The color changed from violet to brownish after complete addition. After 24 h stirring at room temperature, the solution was filtered and evaporated under vacuum to give the desired compound. Yellow crystals were obtained by recrystallization from the mixture of dichloromethane and hexane (1:2). Yield: 0.15 g, 36%. Mp (decomposes) >248 °C. Anal. Calcd for $C_{20}H_{20}N_2O_5V$: C, 57.29; H, 4.81; N, 6.68. Found: C, 57.13; H, 4.67; N, 6.41. Selected IR frequencies (KBr disk, cm^{-1}): 1617 ($\nu_{C=N}$), 986 ($\nu_{V=O}$). Electronic absorption spectrum in CH_2Cl_2 λ_{max} (nm) (ϵ (M^{-1} cm^{-1})): 827 (9.4), 533 (12), 600−610 (30), and 320 (12850). ESR (dichloromethane, 77 and 298 K): g_{av} = 1.9886 and A_{av} = 60. $[\alpha]^{25}_D$ +1.4° (*c* 1, EtOH).

$[(L_3)_2Mn(CH_3COO^-)]$ (9). To a solution of $Mn(OAc)_2{\cdot}4H_2O$ (0.173 g, 1 mmol) in 40 mL of ethanol was added a solution of **3** (0.355 g, 2 mmol) in 10 mL of the same solvent. After 24 h stirring at room temperature, the solution was filtered and evaporated under reduced vacuum to give the complex. Recrystallization from dichloromethane yielded the desired product as brown crystals. Yield: 0.232 g, 42%. Mp 160−162 °C. Anal. Calcd for $C_{22}H_{23}MnN_2O_6$: C, 56.66; H, 4.97; N, 6.00. Found: C, 56.42; H, 4.76; N, 5.74. Selected IR frequency (KBr disk, cm^{-1}): 1617 ($\nu_{C=N}$). Electronic absorption spectrum in CH_2Cl_2 λ_{max} (nm) (ϵ (M^{-1} cm^{-1})): 304 (18310), 660 (111). ESR (solid and dichloromethane, 77 and 298 K): silent. ES-MS: *m*/*z* 446 (M^+), 407 ($M - CH_3COO)^+$.

$[(L_3)_2Co]$ (10). To an ethanol solution (25 mL) of $Co(OAc)_2{\cdot}4H_2O$ (0.177 g, 1 mmol) was added ligand **3** (0.355 g, 2 mmol) dissolved in 10 mL of the same solvent, and stirring was continued for a day at room temperature. Then, the solution was filtered to remove the insoluble impurities and evaporated under reduced vacuum to give a green compound. This compound was crystallized from dichloromethane. Yield: 0.172 g, 42%. Mp (decomposes) >220 °C. Anal. Calcd for $C_{20}H_{20}CoN_2O_4$: C, 58.40; H, 4.90; N, 6.81. Found: C, 58.22; H, 4.68; N, 6.61. Selected IR frequency (KBr disk, cm^{-1}): 1618 ($\nu_{C=N}$). Electronic absorption spectrum in CH_2Cl_2 λ_{max} (nm) (ϵ (M^{-1} cm^{-1})): 646 (541), 346 (5115), 304 nm (5095). ESR (solid and dichloromethane, 77 and 298 K): silent. ES-MS (*m*/*z*): 411 (M^+).

Oxidation Experiments. The catalytic reactions have been carried out in toluene with 1:40:60 catalyst/substrate/oxidant ratio. Catalyst (0.05 mmol) was dissolved in 2 mL of toluene. Styrene

Table 1. Crystallographic Data and Structure Refinement for **3**, **4**, and **8**

	3	**4**	**8**
empirical formula	$C_{10}H_{11}NO_2$	$C_{22}H_{24}N_2O_5V$	$C_{20}H_{20}N_2O_5V$
fw	177.2	447.37	419.32
cryst syst	monoclinic	monoclinic	orthorhombic
space group	$P2_1/n$	$P2_1/c$	$P2_12_12_1$
a (Å)	9.0577(8)	11.8441(6)	8.8894(6)
b (Å)	10.6520	9.2827(5)	11.7764(9)
c (Å)	9.6107(9)	19.8234(10)	18.1078(14)
β (deg)	101.457(2)	93.0430(10)	90
V (Å^3)	908.79(14)	2176.42(19)	1895.6(2)
Z	4	4	4
D(calcd) [Mg/m^3]	1.295	1.365	1.469
abs coeff [mm^{-1}]	0.091	0.491	0.558
obsd reflns [$I > 2\sigma(I)$]	2203	5306	4640
final $R(F)$ [$I > 2\sigma(I)$][a]	0.0652	0.0359	0.0470
wR(F^2) indices [$I > 2\sigma(I)$]	0.1520	0.0893	0.0504
data/restrains/params	2203/8/153	5306/0/299	4640/8/309
GOF on F^2	1.018	1.007	0.810
abs structure param			0.54

[a] Definitions: $R(F_o) = \sum||F_o| - |F_c||/\sum|F_o|$ and $wR(F_o^2) = \{\sum[w(F_o^2 - F_c^2)^2]/\sum[w(F_c^2)^2]\}^{1/2}$.

Table 2. Crystallographic Data and Structure Refinement for **5** and **9**

	5	**9**
empirical formula	$C_{22}H_{24}MoN_2O_6$	$C_{22}H_{23}MnN_2O_6$
fw	508.37	466.36
cryst syst	orthorhombic	monoclinic
space group	$C222_1$	$P2_1/c$
a (Å)	10.585(2)	14.134(8)
b (Å)	14.807(3)	9.851(10)
c (Å)	27.670(6)	15.474(15)
β (deg)	90	107.872(17)
V (Å^3)	4337.0(15)	2050(3)
Z	4	4
D(calcd) (Mg/m^3)	1.557	1.511
abs coeff (mm^{-1})	0.646	0.687
obsd reflns [$I > 2\sigma(I)$]	2681	4406
final $R(F)$ [$I > 2\sigma(I)$][a]	0.0617	0.0720
wR(F^2) indices [$I > 2\sigma(I)$]	0.1445	0.1869
data/restrains/params	2681/0/281	4406/0/280
Goodness of fit on F^2	1.033	1.039

[a] Definitions: $R(F_o) = \sum||F_o| - |F_c||/\sum|F_o|$ and $wR(F_o^2) = \{\sum[w(F_o^2 - F_c^2)^2]/\sum[w(F_c^2)^2]\}^{1/2}$.

(2 mmol) was added followed by the addition of *tert*-butyl hydroperoxide (*t*-BuOOH/H_2O 70:30, 3 mmol) and stirred at room temperature for 24 h. Products were analyzed using gas chromatography.

X-ray Crystallography. Crystallographic data and experimental details for complexes **3**, **4**, **5**, **8**, and **9** are listed in Tables 1 and 2. The diffraction measurements for compounds **3**, **4**, **5**, and **9** were performed on a Siemens R3m/V diffractometer, and for compound **8**, on a Bruker SMART diffractometer with graphite-monochromated Mo Kα radiation (λ = 0.7170 Å). The structures were determined by routine heavy-atom methods using SHELXS-86[17] and Fourier methods and refined by full-matrix least squares with the non-hydrogen atoms anisotropic. Hydrogen atoms with fixed isotropic thermal parameters of 0.07 Å^2 by means of the SHELXL-93 program.[18] Hydrogens were partially located from difference electron-density maps, and the rest were fixed at predetermined positions. Scattering factors were from common sources.

(17) Sheldrick, G. M. *SHELXS-86; Program for Crystal Structure Solution;* University of Göttingen: Germany, 1986.
(18) Sheldrick, G. M. *SHELXL-93*; *Program for Crystal Structure Refinement*; University of Göttingen: Germany, 1993.

Results and Discussion

Syntheses. 2-(4′,4′-Dimethyl-3′,4′-dihydrooxazol-2′-yl)-phenol (**1**),[16] (+)-(4′*R*)-2-(4′-ethyl-3′,4′-dihydrooxazol-2′-yl)-phenol (**2**),[16] and 2-(5,6-dihydro-4*H*-1,3-oxazinyl)phenol (**3**) were prepared from commercially available amino alcohols and 2-hydroxy benzonitriles following the published procedure with minor modification. Ligands **1** and **2** were obtained as brown oil. Ligand (**3**) was obtained as a white solid and structurally characterized by single crystal X-ray crystallography (vide infra).

Oxo−vanadium(IV) (**4**) and oxo−molybdenum(VI) (**5**) complexes were obtained by the reaction of their metal acetylacetonates with ligand (**1**) in absolute alcohol. Oxo−uranium(VI) complexes (**6**, **7**) were synthesized as orange solids by the treatment of uranyl acetate with the corresponding ligand. The novel oxo−vanadium complex (**8**) was obtained by the reaction of vanadium acetylacetonate with oxazine (**3**). Addition of $Mn(OAc)_2{\cdot}4H_2O$ to an ethanolic solution of **3** in 1:2 ratio did not afford the expected 1:2 or 1:3 metal/ligand complex. Instead, it gave the Mn(III) complex (**9**) where the acetate group was coordinated to manganese through two oxygen atoms along with two units of the bidentate oxazine (**3**). This is quite distinct from the reported manganese complexes of bidentate oxazolines where the octahedral coordination of metal is completed by coordination of three units of bidentate oxazoline ligands.[7] It is also worth comparing that the similar reaction of $Mn(OAc)_2{\cdot}4H_2O$ with 2-(4′,4′-dimethyl-3′,4′-dihydrooxazol-2′-yl)phenol in 1:2 ratio gave a complex where one of the oxazoline rings was partially hydrolyzed in the presence of acetic acid eliminated during the reaction.[12] The reaction of $Co(OAc)_2{\cdot}4H_2O$ gave the expected green tetracoordinate Co(II) complex (**10**). The reactions are shown in Scheme 1.

All the complexes are highly soluble in common organic solvents such as dichloromethane and chloroform except the oxo−molybdenum complex (**5**) which is soluble only in strongly coordinating solvents such as DMSO and DMF and is sparingly soluble in acetonitrile and methanol. All are stable enough to handle in air and can be stored for a long period. Complexes **4**, **5**, **8**, and **9** were structurally characterized by single crystal X-ray diffraction (vide infra). The complexes (**6** and **7**) were recrystallized from a methanol and acetonitrile mixture (1:1); however, attempts to get X-ray quality crystals were unsuccessful.

Description of Structures. The important bond lengths and bond angles that cover the primary coordination sphere are summarized in Tables 3 and 4.

Crystal Structure of 3. The crystal structure of **3** is shown in Figure 1. An intramolecular $N^1\cdots H^1$ [1.611 Å] hydrogen bond exists between the imine nitrogen of the oxazine ring and the hydrogen attached to the phenoxo group leading to the formation of another six-membered heterocyclic ring consisting of four different atoms i.e., carbon, hydrogen, oxygen, and nitrogen. The $N^1\cdots H^1$ distance is shorter than the sum of the van der Waals radii (1.75 Å) and longer than the single bond covalent radii (1.12 Å). The molecule is almost planar which may be due to the formation of a chelate

Scheme 1

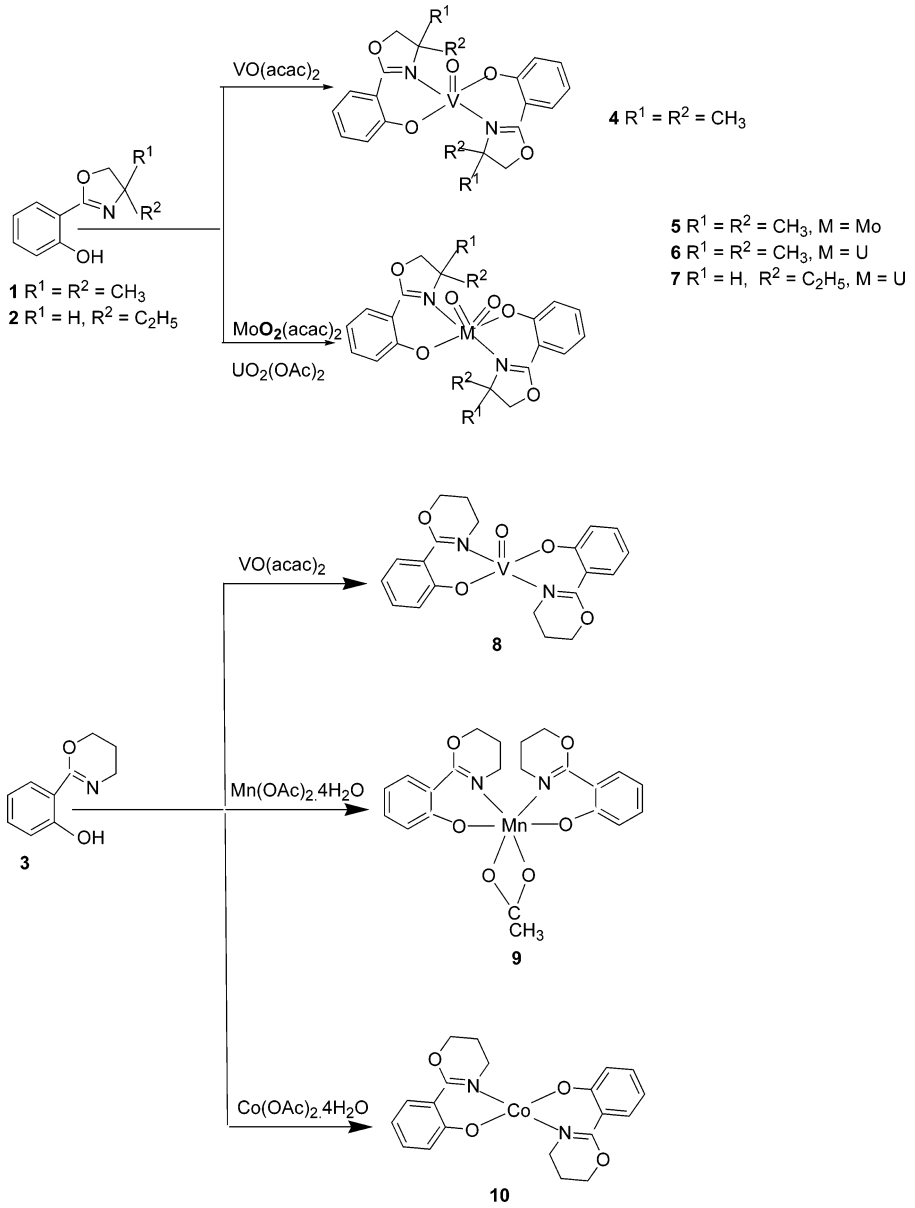

ring via intramolecular hydrogen bonding. In addition, intermolecular $O^{1a}\cdots H^1$ [1.611 Å] interactions exist the between phenoxo oxygen and the hydrogen of the methylene group present in the oxazine ring. The bond angle of $O^1-H^1\cdots N^1$ is 159.91°. The torsion angles of $N^1-C^7-C^6-C^1$ and $C^1-O^1-H^1\cdots N^1$ are 0.90° and 6.93°, respectively.

Crystal Structures of 4 and 8. The crystal structures of **4** and **8** are depicted in Figures 2 and 3, and both complexes are isostructural. However, the interesting feature of structure **8** is that it crystallizes in a chiral space group $P2_12_12_1$ whereas complex **4** crystallizes in the $P2_1/c$ space group. The geometry around the vanadium center is common [for oxo−vanadium(IV) complexes] distorted square pyramidal with two units of bidentate (N, O) oxazoline/oxazine ligands *trans* coordinated in equatorial plane and axial terminal oxygen atom. The bond lengths and angles of primary coordination sphere are comparable to the other reported oxo−vanadium-(IV) complexes.[19] A close comparison of structure **8** with bis[2-(2′-oxyphenyl)-2-oxazolinato]oxo−vanadium(IV) (**11**)[13] reveals that the V═O [1.587(2) Å] and V−O distances [1.883(2); 1.883(2) Å] of **8** are slightly shorter than the corresponding distances [1.594(1) Å and 1.931(1); 1.926(1) Å, respectively] reported for **11**. In contrast, V−N distances [2.086(3); 2.079(3) Å] of **8** are slightly longer than the respective distances [2.068(1); 2.061(1) Å] of **11**. The O═V−O and N−V−N angles are significantly longer, while O═V−N and O−V−O angles are slightly shorter than the respective angles of **11** (see Table 5). The displacement of the vanadium from the plane defined by the ligand donor atoms in **8** is 0.55 Å, whereas in bis[2-(2′-oxyphenyl)-2-oxazolinato]oxo−vanadium(IV) it is 0.57 Å. The V═O, V−N, and V−O bond distances are also in good agreement with bis[(4′*R*)-2-(4′-ethyl-3′,4′-dihydroxazol-2′-yl)phenola-

(19) (a) Vlahos, A. T.; Tolis, E. I.; Raptopoulou, C. P.; Tsohos, A.; Sigalas, M. P.; Terzis, A.; Kabanos, T. A. *Inorg. Chem.* **2000**, *39*, 2977. (b) Hagen, H.; Bezemer, C.; Boersma, J.; Koojiman, H.; Lutz, M.; Spek, A. L.; van Koten, G. *Inorg. Chem.* **2000**, *39*, 3970. (c) Hagen, H.; Barbon, A.; van Faassen, E. E.; Lutz, B. T. G.; Boersma, J.; Spek, A. L.; van Koten, G. *Inorg. Chem.* **1999**, *38*, 4079.

Table 3. Significant Bond Lengths (Å) and Angles (deg) for **3**, **4**, and **8**

3			
O(I)−C^1	1.349(2)	O(I)−H^1	0.95(3)
O^2−C^7	1.334(2)	O^2−C(8B)	1.467(5)
O^2−C(8A)	1.475(5)	N(I)−C^7	1.282(2)
N(I)−C(10A)	1.471(5)	N(I)−C(10B)	1.474(5)
C^1−O^1−H^1	100.2(17)	C^7−O^2−C(8B)	115.1(4)
C^7−O^2−C(8A)	114.9(5)	C^7−N^1−C(10A)	122.9(3)
C^7−N^1−C(1B)	117.0(4)	C(10A)−N^1−C(10B)	6.8(7)
C^1−O^1−H^1	100.2(17)	O^1−C^1−C^2	118.7(2)

	4	**8**
O−V	1.5934(12)	1.587(2)
O(IB)−V	1.9094(12)	1.883(2)
O(1A)−V	1.9173(11)	1.883(2)
N(IA)−V	2.1021(13)	2.086(3)
N(IB)−V	2.1063(13)	2.079(3)
O−V−O(1B)	116.05(6)	116.27(12)
O−V−O(1A)	114.31(6)	116.05(17)
O(1A)−V−O(1B)	129.64(5)	127.67(11)
O−V−N(1A)	97.55(6)	97.11(13)
O(1B)−V−N(1A)	86.99(5)	87.20(12)
O(1A)−V−N(1A)	85.70(5)	86.30(11)
O−V−N(1B)	97.05(6)	97.74(14)
O(1A)−V−N(1B)	89.34(5)	86.42(12)
O(1B)−V−N(1B)	85.60.[5]	87.02(13)
N(1A)−V−N(1B)	165.36(5)	165.14(13)
O2A−C7A	1.3516(19)	1.342(5)
O2B−C7B	1.350(2)	1.332(5)
O2A−C8A	1.457(2)	1.413(18)
O2B−C8B	1.457(2)	1.36(2)
N1A−C7A	1.295(2)	1.281(5)
N1B−C7B	1.297(2)	1.273(6)
N1A−C10A	1.503(2)	1.55(2)
N1B−C10B	1.503(2)	1.45(2)

to],[4] bis[(4′*S*)-2-(4′-dihydroxazol-2′-yl)phenolato]oxo−vanadium(IV)[4] complexes, and vanadium(IV) bis(phenolate) complexes having the VN_2O_4 chromophore.[19] Nevertheless, the bite angles (O═V−O, O−V−O, O═V−N, and N−V−N) of **4** and **8** are significantly different from each other and also from the recently reported oxo−vanadium(IV) complexes containing oxazoline moieties (Table 5).

Crystal Structure of 5. The molecular structure of **5** is displayed in Figure 4. The geometry of the molybdenum(VI) center is distorted octahedral which is completed by the coordination of two bidentate oxazoline ligands and two terminal oxo groups. Mo═O distances (1.684 Å) are within the range reported for typical oxo−molybdenum complexes (1.668−1.694 Å).[20] The Mo−O, Mo−N, C−O, and C−N distances and bite angles O−Mo−O, O−Mo−N, and N−Mo−N are as reported for the similar type of oxo−molybdenum compounds.[21] In particular, the bond angles of O(2A)#1−Mo(1A)−O(2A) (155.5(6)°) and N(1A)#1−Mo(1A)−N(1A) (84.7(5)°) are smaller and larger than the respective angles of dioxo-bis[(4′*R*)-2-(4′-ethyl-3′,4′-dihydroxazol-2′-yl)phenolato]molybdenum(VI),[5] 158.81(7)° and 75.37(6)°, respectively. The Mo−N bond distance [N(IA)−Mo(1A), 2.1021(13) Å] is also shorter than the respective distance [2.334(2) Å] in dioxo-bis[(4′*R*)-2-(4′-ethyl-3′,4′-dihydroxazol-2′-yl)phenolato]molybdenum(VI).

Crystal Structure of 9. The molecular structure of complex **9** with the atom numbering scheme is depicted in Figure 5. The Mn(III) complex consists of a Jahn−Teller distorted octahedral MnN_2O_4 chromophore. The distorted octahedral structure has the equatorial plane consisting of N(1A), N(1B) from the oxazoline rings and O^1, O^2 of the acetate group in addition to the phenoxo groups in axial positions. The structure has a compressed Jahn−Teller axis along the O(1A)−Mn−O(1B) bonds which is revealed by short Mn−O(1A) (1.861(3) Å) and Mn−O(1B) (1.866(3) Å) bond distances compared to Mn−O^2 (2.114(4) Å) and Mn−O^1 (2.262(4) Å) bond distances, as is to be expected for a Jahn−Teller distorted d^4 ion. The observation of axial compressed distortion in this complex is very unusual, since most of the other known Mn^{III} containing oxazoline moieties exhibit axial elongation.[7a−c] The Mn−N ((2.086(4) and 2.106(4) Å) bond distances of the structure (**9**) are almost equal which is unlike the reported manganese complexes of 2-(2′-hydroxyphenyl)oxazolines where the Mn−N distances (2.033−2.086 and 2.192−2.238 Å) are deviated (>0.1 Å) from each other.[7b,d,12] However, the equal Mn−N distances were observed where the octahedral coordination is completed by two axially coordinated solvent molecules.[7a−c] The bite angle O^1−Mn−O^2 (59.41(4)°) is the smallest ever reported for Mn^{III} complexes. The O−Mn−O and O−Mn−N bond angles where the oxygen atoms from the acetate group are involved deviate significantly (∼4−14°) from the other reported manganese complexes having a MnN_2O_4 core.[7c,12]

Common Structural Features. The C^7−O (1.326−1.352 Å) and C^7−N (1.262−1.295 Å) bond lengths for **3**, **4**, **5**, **8**, and **9** are significantly shorter than the C^8−O (1.413−1.475) and C^{10}−N (1.40−1.55) bond lengths, respectively. This indicates the existence of double bond character both in C^7−O and C^7−N as reflected in the resonance structure in Chart 1. The C^7−O (1.342(5) Å) and C^7−N (1.281(5) Å) bond lengths of **8** are almost similar to the corresponding distances of bis[2-(2′-oxyphenyl)-2-oxazolinato]oxo−vanadium(IV) (**11**),[13] 1.347(2) and 1.284(2) Å, respectively. This suggests that the change in ring size has no influence on the resonance structure as resonance structure B is more stabilized in both the complexes. However, C^7−O and C^7−N bond lengths of **8** and **11** are slightly shorter than the corresponding distances 1.3516(19) and 1.295(2) Å, respectively, in complex **4**. This indicates the existence of some double bond character of C^7−O and C^7−N which are stronger in complexes **8** and **11** than in complex **4**. This may be due to the stabilization of resonance structure B (Chart 1) in complexes **8** and bis[2-(2′-oxyphenyl)-2-oxazolinato]-oxo−vanadium(IV)[13] than in **4** which may be attributed to the absence of electron releasing methyl groups at the carbon atom adjacent to the nitrogen in the oxazoline/oxazoline ring.

Spectroscopic Properties. ^{1}H and ^{13}C NMR spectra were obtained for the ligand (**3**) and for the diamagnetic complexes **5**, **6**, and **7** as well. ^{1}H NMR of complexes **5**, **6**, and **7** showed the disappearance of the phenoxo-OH proton. However, other protons exhibited only slight changes in the chemical shifts

(20) (a) Harben, S. M.; Smith, P. D.; Beddoes, R. L.; Collison, D.; Garner, C. D. *J. Chem. Soc., Dalton Trans.* **1997**, 2777. (b) Hishaw, C. J.; Peng, G.; Singh, R.; Spence, J. T.; Enemark, J. H.; Bruck, M.; Kristozki, J.; Merbs, S. L.; Ortega, R. B.; Wexler, P. A. *Inorg. Chem.* **1989**, *28*, 4483.

(21) Lee, H. K.; Wong, Y.-L.; Zhou, Z.-Y.; Zhang, Z.-Y.; Ng, D. K. P.; Mak, T. C. W. *J. Chem. Soc., Dalton Trans.* **2000**, 539.

Table 4. Significant Bond Lengths (Å) and Angles (deg) for **5** and **9**

5			
O(1A)−Mo(1A)	1.684(11)	O(3A)−Mo(1A)	1.933(11)
N(IA)−Mo(1A)	2.385(13)	O(1A)#1−Mo(1A)−O(1A)	105.2(8)
O(1A)#1−Mo(1A)−O(3A)	95.5(5)	O(1A)−Mo(1A)−O(3A)	99.3(5)
O(3A)#1−Mo(1A)−O(3A)	155.5(6)	O(1A)#1−Mo(1A)−N(1A)#1	85.3(5)
O(1A)−Mo(1A)−N(1A)#1	168.3(5)	N(1A)#1−Mo(1A)−O(3A)#1	77.6(4)
N(1A)#1−Mo(1A)−O(3A)	84.3(4)	N(1A)#1−Mo(1A)−N(1A)	84.7(5)
O2A−C8A	1.45(2)	O2A−C7A	1.326(16)
N1A−C10A	1.53(2)	N1A−C7A	1.259(18)
9			
Mn−O(1A)	1.866(3)	Mn−O(1B)	1.861(3)
Mn−N(1A)	2.106(4)	Mn−N(1B)	2.086(4)
Mn−O^2	2.114(4)	Mn−O^1	2.262(4)
Mn−O(1A)	1.866(3)	Mn−O(1B)	1.861(3)
O(1B)−Mn−O(1A)	177.48(13)	O(1B)−Mn−N(1B)	86.97(13)
N(1B)−Mn−O(1A)	91.25(12)	N(1A)−Mn−O(1A)	87.33(14)
N(1B)−Mn−N(1A)	99.34(15)	O(1B)−Mn−O^2	91.23(14)
O^2−Mn−O(1A)	91.04(14)	N(1B)−Mn−O^2	160.26(14)
O^2−Mn−N(1A)	100.35(15)	O(1B)−Mn−O^1	88.22(14)
O^1−Mn−O(1A)	93.87(14)	N(1B)−Mn−O^1	100.87(14)
O^1−Mn−N(1A)	159.72(14)	O^2−Mn−O^1	59.41(14)
O2A−C7A	1.349(6)	O2A−C8A	1.445(6)
O2B−C7B	1.340(5)	O2B−C8B	1.460(5)
N1A−C7A	1.288(6)	N1A−C10A	1.482(6)
N1B−C7B	1.287(6)	N1B−C10B	1.485(5)

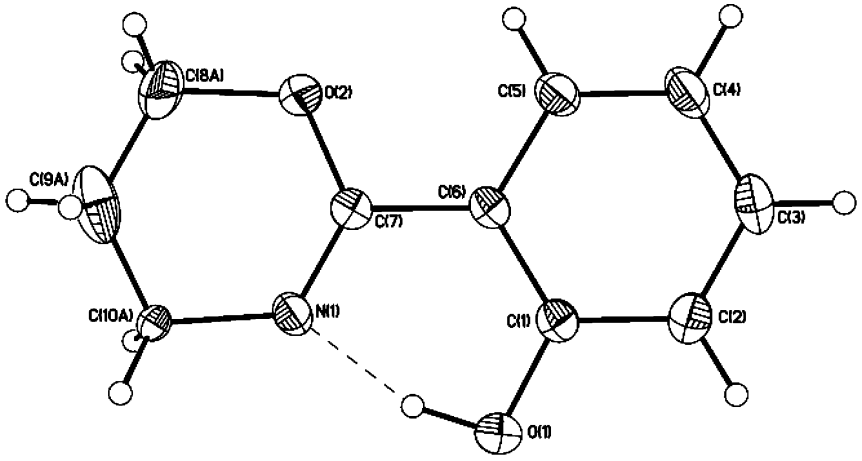

Figure 1. ORTEP diagram of ligand **3**.

Table 5. Comparison of Bond Angles of Oxovanadium(IV) Complexes Containing Oxazoline Moieties

bond angles	**4**	**8**	**11**[a]	**12**[b]	**13**[c]
O−V−O(1A)	116.05(6)	116.05(12)	108.41(5)	110.9(3)	112.3(2)
O−V−O(1B)	114.31(6)	116.27(12)	108.81(5)	110.9(3)	112.3(2)
O(1A)−V−O(1B)	129.64(5)	127.67(11)	142.79(5)	139.8(2)	135.3(2)
O−V−N(1A)	97.55(6)	97.11(13)	104.73(6)	103.9(3)	101.7(2)
O−V−N(1B)	97.05(6)	97.74(14)	103.79(5)	103.9(3)	101.7(2)
O(1A)−V−N(1A)	85.70(5)	87.20(12)	85.28(5)	86.40(2)	85.20(2)
O(1A)−V−N(1B)	89.34(5)	86.42(12)	85.25(5)	86.40(2)	85.20(2)
O(1B)−V−N(1A)	86.99(5)	86.30(11)	85.23(5)	85.30(2)	85.40(2)
O(1B)−V−N(1B)	85.60(5)	87.02(12)	86.21(5)	85.30(2)	85.40(2)
N(1A)−V−N(1B)	165.36(5)	165.14(13)	151.47(5)	153.30(2)	155.8(2)

[a] Bis[2-(2′-oxyphenyl)-2-oxazolinato]oxovanadium(IV).[13] [b] Bis[(4′*R*)-2-(4′-ethyl-3′,4′-dihydroxazol-2′-yl)phenolato-*N*,*O*]oxovanadium(IV).[4a] [c] Bis-[(4′*S*)-2-(4′-dihydroxazol-2′-yl)phenolato-*N*,*O*]oxovanadium.[4a]

compared with the corresponding unbound ligands. The ^{13}C NMR spectra were also not informative as there are no significant changes in chemical shifts between the complexes and the free ligands.

The $\nu_{C=N}$ vibrations for all complexes (**4**−**10**) are found in the range 1610−1640 cm^{-1}, and are shifted at least by 20−30 cm^{-1} to a lower frequency compared to the free ligands, indicating that the imine nitrogen of the oxazoline and oxazine rings is strongly coordinated to the metal center. The $\nu_{V=O}$ bands observed for the oxo−vanadium complexes (**4** and **8**) are in the range 970−990 cm^{-1} and suggest the presence of a square pyramidal environment around the metal center.[4a,13] The $\nu_{Mo=O}$ (916−962 cm^{-1}) observed for complex **5** is within the range of reported values of asymmetric and symmetric Mo═O stretching frequencies.[5,22] The $\nu_{U=O}$ vibrations in the range 891−912 cm^{-1} for complexes **6** and **7** are characteristic of the O═U═O stretching frequencies.[23] The other bands in the IR region are assigned to the vibrational signals of the bound ligands.

Electronic spectra of the complexes were recorded in dichloromethane solution. Three spin allowed transitions in

(22) Gonclaves, I. S.; Santos, A. M.; Romão, C. C.; Lopes, A. D.; Rodriguez-borges, J. E.; Pillinger, M.; Ferreira, P.; Rocha, J.; Kühn, F. E. *J. Organomet. Chem.* **2001**, *626*, 1.

(23) (a) Rao, P. V.; Rao, C. P.; Sreedhara, A.; Wegelius, E. K.; Rissanen, K.; Kolehmainen, E. *J. Chem. Soc., Dalton Trans*. **2000**, 1213. (b) Singnorini, O.; Dockal, E. R.; Castellano, G.; Oliva, G. *Polyhedron* **1996**, *15*, 245. (c) Francyzk, T. S.; Czerwinski, K. R.; Raymond, K. N. *J. Am. Chem. Soc*. **1992**, *114*, 8138.

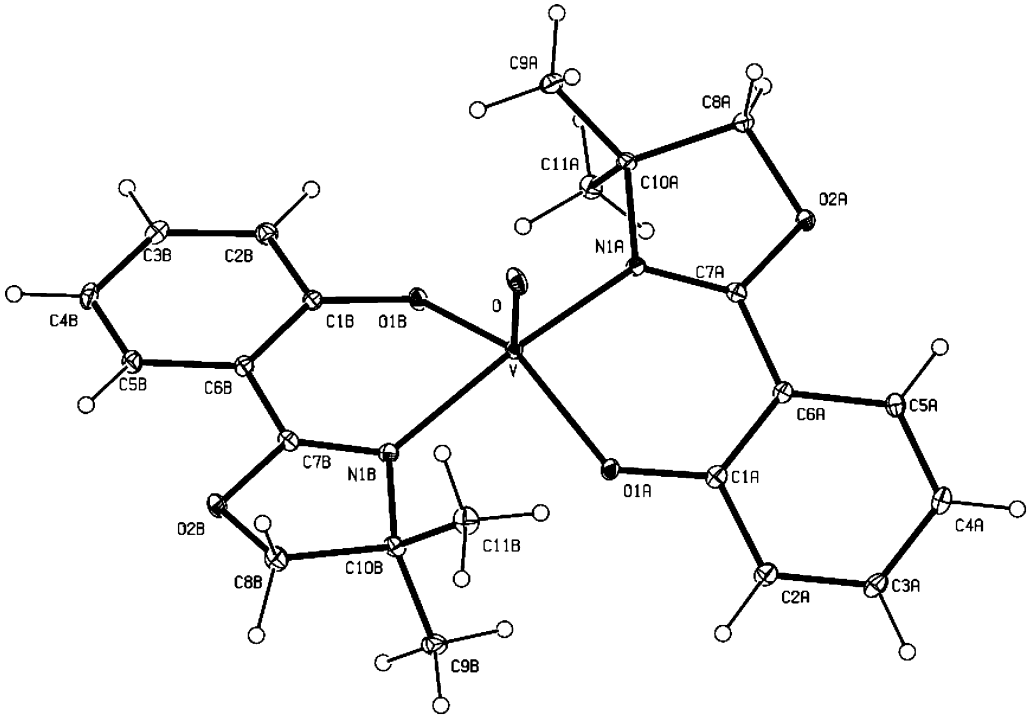

Figure 2. ORTEP diagram of complex **4**.

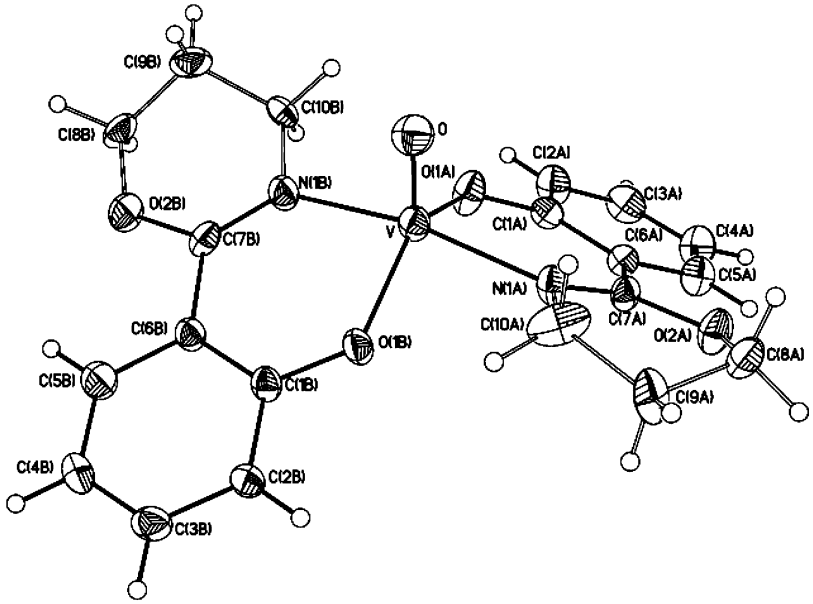

Figure 3. ORTEP diagram of complex **8**.

the range 540−550 nm (ϵ = 33 M^{-1} cm^{-1}), 600−620 nm (ϵ = 50 M^{-1} cm^{-1}), and 800−850 nm (ϵ = 59 M^{-1} cm^{-1}) observed for complex **4** can be assigned to $^2B_2$ (d_{xy}) → $^2A_1$ (d_{z^2}), $^2B_2$ → $^2B_1$ ($d_{x^2} - d_{y^2}$), and $^2B_2$ → ^2E (d_{xz}, d_{yz}) transitions, respectively.[24] The spectrum also exhibits a fourth band in the ultraviolet region 325−330 nm (ϵ = 8100 M^{-1} cm^{-1}) which can be assigned as a ligand−metal charge-transfer transition. Similarly, three weak features in the region 827 nm (ϵ = 9.4 M^{-1} cm^{-1}), 533 nm (ϵ = 12 M^{-1} cm^{-1}), and 600−610 nm (ϵ = 30 M^{-1} cm^{-1}) with very low intensity, and one band at 320 nm (ϵ = 12850 M^{-1} cm^{-1}), are observed for **8**. The electronic spectrum of the manganese complex (**9**) is dominated by the peak centering at 304 nm (ϵ = 18310 M^{-1} cm^{-1}) attributable to the σ(N) → Mn(III) LMCT transition. One shoulder that appears at 660 nm (ϵ = 111 M^{-1} cm^{-1}) may be attributed to the ligand field transition. Only charge-transfer transitions at 296 nm (ϵ = 1070 M^{-1} cm^{-1}) for **5**, 305 nm (ϵ = 17710 M^{-1} cm^{-1}) for **6**, at 306 nm (ϵ = 10959 M^{-1} cm^{-1}) and 350 nm (ϵ = 5163 M^{-1} cm^{-1}) for **7** were observed. For complex **10**, a broad peak at 646 nm (ϵ = 541 M^{-1} cm^{1}) may be attributed to a d−d transition. The high intensity of this band may be due to intensity borrowing from the nearby charge-transfer band. The peaks in the high-energy region, 346 nm (ϵ = 5115 M^{-1} cm^{1}) and 304 nm (ϵ = 5095 M^{-1} cm^{1}), can be assigned to the charge-transfer transitions.

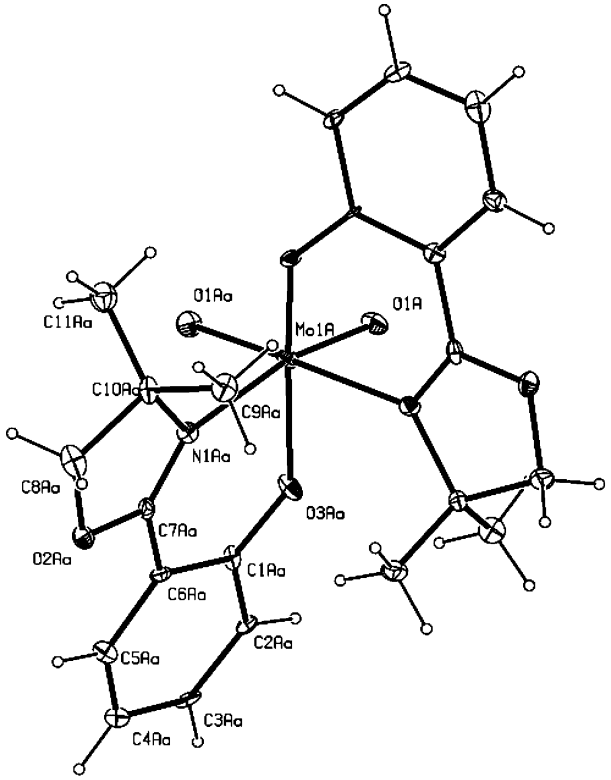

Figure 4. ORTEP diagram of complex **5**.

EPR spectra of oxo−vanadium complexes (**4** and **8**) in dichloromethane showed the eight line spectra with hyperfine splitting factor [$g_{av} = 1.9777$ for **4** and $g_{av} = 1.9886$ for **8**] and hyperfine coupling constant [$A_{av} = 100$ for **4** and $A_{av} = 60$ for **5**] as expected for a d^1 system at room temperature and liquid nitrogen temperature as well. As expected, Mn(III) complex **9** did not show any ESR signal when the spectrum was recorded in the solid state as well as in dichloromethane at room temperature and liquid nitrogen temperature.[2d,12] The EPR spectrum of complex **10** also did not give any signal either at room temperature or at liquid nitrogen temperature in solution as well as in the solid state which may be attributed to the very short spin lattice relaxation time of Co(II) ions.[25]

Mass Spectrometry. Mass spectra were recorded for complexes **3**, **4**, **6**, **7**, **9**, and **10** to identify the constitution of the products under mass spectrometric conditions. Molecular ion peaks with 100% intensity were observed for complexes **3** and **10**, whereas for complexes **4**, **6**, **7** and **9** they were observed with medium intensity. For the complex **4**, the peak at *m*/*z* 257 corresponding to $[VOL]^+$ was observed. In complex **6**, the peak observed at *m*/*z* 192 can be assigned to the $[L]^+$ fragment. The peaks at *m*/*z* 460 and at 192 corresponding to $[UO_2L]^+$ and $[L]^+$ fragments were observed in the case of **7**. The mass peak observed at *m*/*z* 407 with 100% intensity for complex **9** corresponding to the $[MnL_2]^+$ species indicates the dissociation of acetate ion in solution. Observation of mass peaks higher than the molecular weights for complexes **6** and **10** provides evidence for the formation of higher aggregates in addition to the monomeric forms.

Electrochemistry. Cyclic voltammograms of complexes **4**−**10** were recorded in acetonitrile in the potential range −1.5 to +2.0 V versus Ag/AgCl reference electrode using tetrabutylammonium perchlorate as supporting electrolyte. Complex **4** exhibits irreversible oxidation peaks at +0.47, +0.92, and +1.26 V. The irreversible oxidation peaks suggest that the V^V complex is unstable, and are consistent with the exclusive formation of the V^{IV} complex. Similarly, complex **8** also shows three irreversible oxidation peaks at +0.15, +0.61, and +1.1 V when tetrabutylammonium hexaflurophosphate was used as a supporting electrolyte while it gives only one quasireversible oxidation peak at 0.90 V when tetrabutylammonium perchlorate or tetrabutylammonium bromide was used as supporting electrolyte. The potentials are similar to those observed for the mixed complexes of the N_3O_3/NO_5 core.[26] For complex **9**, the irreversible oxidation processes were observed at +0.71 and 1.17 V. The redox couple corresponding to Mn^{III}/Mn^{II} was not observed up to −2.0 V. The irreversible oxidation peaks indicate that the Mn^{IV} and Mn^V complexes are unstable, and this is consistent with the exclusive formation of Mn^{III} complexes in synthetic reactions. Other complexes (**5**−**7** and **10**) did not show any well-defined response in this potential range −1.5 to +2.0 V. Blank scans of the unbound ligands under similar conditions show no redox activity within this potential range.

Oxidation of Styrene. Recently, nickel, palladium, and manganese complexes of oxazoline ligands have been reported to catalyze the epoxidation of styrene with *tert*-butyl hydroperoxide or NaOCl.[2d,7] Similarly, oxo−vanadium and −molybdenum complexes containing oxazoline moieties were used for epoxidation of olefins.[4,5] These results prompted us to test the activity of complexes **4**−**6** containing achiral oxazoline, **8** and **9** containing oxazine, and **7** and **12** having chiral oxazoline units for the oxidation of styrene using catalytic amounts of the corresponding complex with *tert*-butyl hydroperoxide as oxidant under a standard set of conditions. The results are summarized in Table 6. The activity obtained with the closely related oxo−vanadium complexes **4**, **8**, and **12** is relatively high (26.3−33% conversion of the styrene) compared to that of complexes **5**−**7** and **9** which have other transition metals. The low activity of some complexes (**5**, **7**, and **9**) is probably due to hexacoordination of the metal center in these complexes. This might be disadvantageous for the oxidant and the substrate to access the metal coordination sites whereas oxo−vanadium complexes (**4**, **8**, and **12**) which are pentacoordinated can be more accessible for coordination of the oxidant and substrate. Among the oxo−vanadium complexes, complex **8** having the oxazine moiety exhibits better catalytic activity

(24) Ballhausen, C. J.; Gray, H. B. *Inorg. Chem.* **1962**, *1*, 111.
(25) (a) March, R.; Clegg, W.; Coxall, R. A.; Cucurull-Sánchez, L.; Lezama, L.; Rojo, T.; González-Duarte, P. *Inorg. Chim. Acta* **2003**, *353*, 129. (b) Weil, J. A.; Bolton, J. R.; Wertz, E. *Electron Spin Resonance*: *Elementary Theory and Practical Applications*, 2nd ed.; Wiley: New York, 1994.
(26) (a) Chakravarty, J.; Dutta, S.; Chandra, S. K.; Basu, P.; Chakravorty, A. *Inorg. Chem.* **1993**, *32*, 4249. (b) Mondal, S.; Dutta, S.; Chakravorty, A. *J. Chem. Soc., Dalton Trans.* **1995**, 1115.

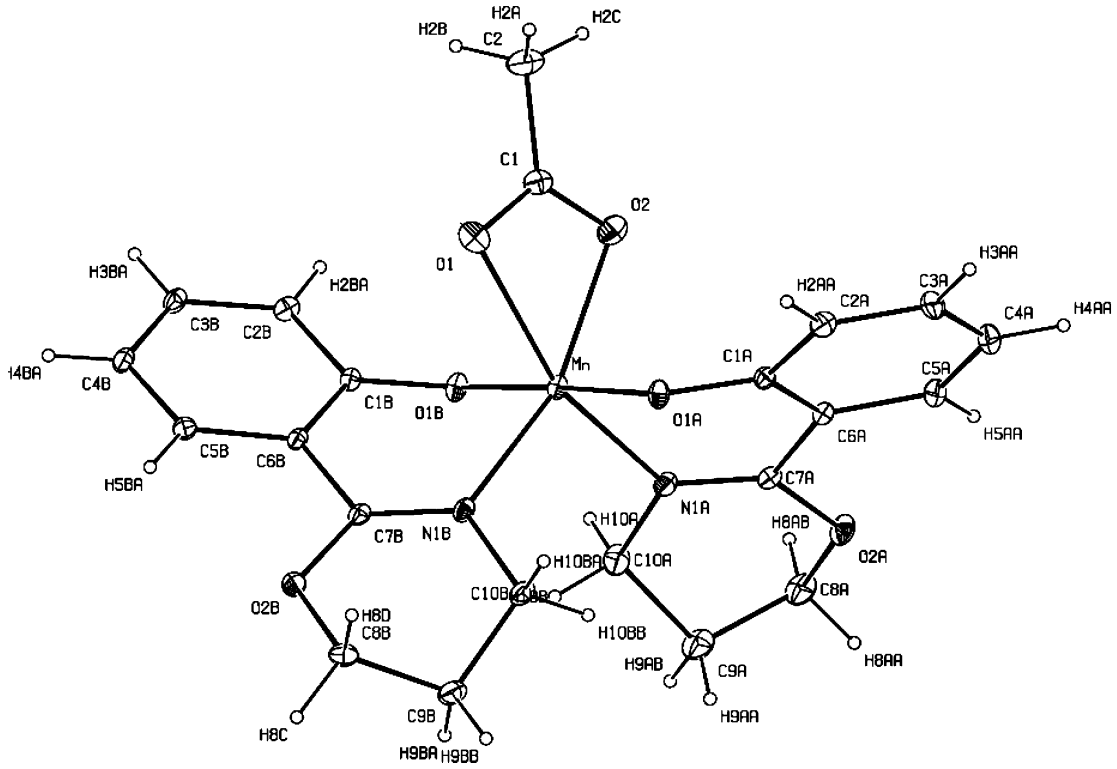

Figure 5. ORTEP diagram of complex **9**.

Table 6. Metal-Catalyzed Styrene Oxidation Reaction

catalyst	time (h)	*T*	conversion (%)	epoxide (%)	benzaldehyde (%)
4	24	RT	26.3		26.3
5	24	RT			
6	24	RT	5.8		5.8
7	24	RT	2.5		2.5
8	24	RT	33		33
9	24	RT	8.2		8.2
12[a]	24	RT	28.4	9.2	19.2

[a] Bis[(4′*R*)-2-(4′-ethyl-3′,4′-dihydroxazol-2′-yl)phenolato-*N*,*O*]oxovanadium(IV).[4a]

(33%) than complexes **4** (26.3%) and **12** (28.4%) which have the oxazoline moiety. This difference in activity may probably be due to the steric influence of the ligands.

Conclusion

Oxo−vanadium, oxo−molybdenum, and the first examples of oxo−uranium complexes with 2-(4′,4′-dimethyl-3′-4′-dihydroxazol-2′-yl)phenol and oxo−vanadium, manganese and cobalt complexes with a novel oxazine, 2-(5,6-dihydro-4*H*-1,3-oxazolinyl)phenol, have been successfully prepared and characterized. Complex **8** crystallizes in the chiral $P2_12_12_1$ space group. Compared to complex **4**, the shorter distance between the vanadium and nitrogens in complex **8** may be due to the absence of electron releasing methyl groups at the carbon atom adjacent to the nitrogen in the oxazine ring. Also, complex **8** gave better conversion of styrene (33%) than other reported oxo−vanadium complexes under identical experimental conditions. In manganese complex **9**, the octahedral coordination is completed by the coordination of the acetate molecule via two oxygen atoms in addition to the two bidentate oxazine ligands whereas in other reported manganese complexes octahedral coordination is completed either by three bidentate ligands or by two bidentate ligands and one oxidized oxazoline ring via two oxygen atoms. This contrasting behavior compared to that of other reported manganese complexes where 1:3 or 1:2 metal/ligand complex formation has been reported may be due to the steric influence of the six-membered oxazine ring present in the system.

Acknowledgment. We are grateful to the Department of Science and Technology (DST), New Delhi. Thanks are due to RSIC, Central Drug Research Institute (CDRI), Lucknow, for providing mass spectra.

Supporting Information Available: Crystallographic data for **3**−**5**, **8**, and **9** comprising a complete list of final atomic coordinates, bond lengths and angles, and hydrogen atom coordinates. This material is available free of charge via the Internet at http://pubs.acs.org.

IC0352093